Dissociation lifetime studies of doubly deprotonated angiotensin peptides

G. Aravind, L. Lammich, and L. H. Andersen
Institute of Physics and Astronomy, University of Aarhus, DK-8000 Aarhus C, Denmark
(Received 7 September 2008; published 15 January 2009)

The doubly deprotonated [Asn, Val^5] angiopeptide, in the gas phase, was irradiated with 266 nm photons. The time of flight (TOF) of the products formed following photoabsorption, namely, the monoanion and neutral fragments, was recorded with submicrosecond time resolution. Monte Carlo simulations of the TOF of the neutral fragments indicate that the dissociation occurs faster than 100 ns. A similar experiment performed on the Val^5 angiopeptide also yielded a dissociation time shorter than 100 ns. We suggest dissociation mechanisms that account for the different number of photons required for the release of CO_2.

DOI: 10.1103/PhysRevE.79.011908 PACS number(s): 87.64.−t

I. INTRODUCTION

The oligopeptide angiotensin plays an important role in biological systems by increasing blood pressure through vasoconstriction, regulating the release of aldosterone, and influencing the neural system and renal blood flow. In general, the chemical reactions involving peptides critically determine the response of biological systems to a variety of external stimulations. To study such responses in biological systems one needs knowledge of the electronic energy levels, intramolecular vibrational redistribution (IVR) mechanisms, and dissociation pathways for these large biomolecules. The intrinsic physical and chemical properties of the biomolecules are best studied in the gas phase where perturbative effects from environments are avoided [1–7].

Techniques based on photoabsorption are convenient for probing the physical and chemical properties of molecular systems due to the well-defined energy of the photons and the excellent timing properties of lasers. Photoexcitation of large molecules would usually result in redistribution of the excitation energy among the internal degrees of freedom [8]. The signal transmission along the length of a polypeptide from the site of energy absorption to the site of the chemical reaction center can be surprisingly efficient in spite of energy dissipation mechanisms, such as the IVR. Weinkauf *et al.* [9,10] have studied the photodissociation of polypeptides and have reported fast fragmentation pathways that circumvent IVR. On the other hand, Liftshitz *et al.* [11] in their time-resolved photodissociation studies report a statistical fragmentation pathway in peptides with decay rates correlating well with the length of the peptide chain and the energy deposited at the absorption site. Photodetachment and dissociation of peptide anions have been studied using ion traps, where the parent and the fragment ion signals are recorded after photoexcitation [12–16]. Dugourd *et al.* [13] have recently studied the photodetachment of two variants of doubly deprotonated angiopeptides, namely, the [Asn, Val^5] and the Val^5 dianions, under UV radiation.

The [Asn, Val^5] dianion is deprotonated at the phenoxy site of tyrosine and at the carboxylate site of phenylalanine, as shown in Fig. 1. The Val^5 peptide is deprotonated at the two carboxylate positions attached to aspartic acid and the phenylalanine. The two peptide variants have an absorption resonance below 300 nm due to the π-π^* transition at the aromatic site of tyrosine (Y) [12,17]. The single electron detachment that follows the photoabsorption can have two different pathways: The electronically excited dianion might deexcite by internal conversion where the resulting "hot" dianion eventually undergoes electron detachment, or the excited dianion may undergo curve crossing to an autoionizing state [12,18]. If the autoionizing state is below the repulsive Coloumb barrier (RCB), the detaching electron will have to tunnel through the barrier before reaching the continuum. Wang *et al.* [18] have studied such electron tunneling across the RCB in the case of linear carboxylic dianions with varying charge separations.

It has been established that UV photoabsorption results in single-electron detachment followed by the release of a neutral CO_2 fragment [13]. The monoanion yield was determined to be due to a single-photon process for both variants, while the yield of CO_2 was due to a two-photon process for [Asn, Val^5] and a single-photon process for Val^5. It is important to note that the electron-detachment energy for the phenoxy anion (2.25 eV) [19] is less than that for the carboxylate anion (3.48 eV) [20], and hence the energy remnant after the monoanion formation is more in the case of [Asn, Val^5] than Val^5. The observed requirement for the second photon to trigger the dissociation in [Asn, Val^5] was earlier explained by a possible charge transfer model [12]. However, the understanding of the dissociation process would remain

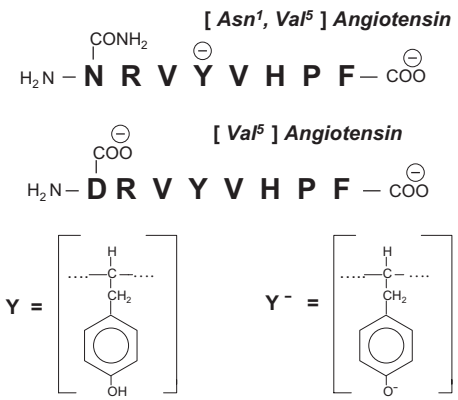

FIG. 1. The amino acid sequence for Val^5 and [Asn, Val^5] angiopeptides, indicating the location of the negative charges. The single alphabetic representation for amino acids is followed. In both the peptides it is tyrosine or tyrosylate that is excited at 266 nm.

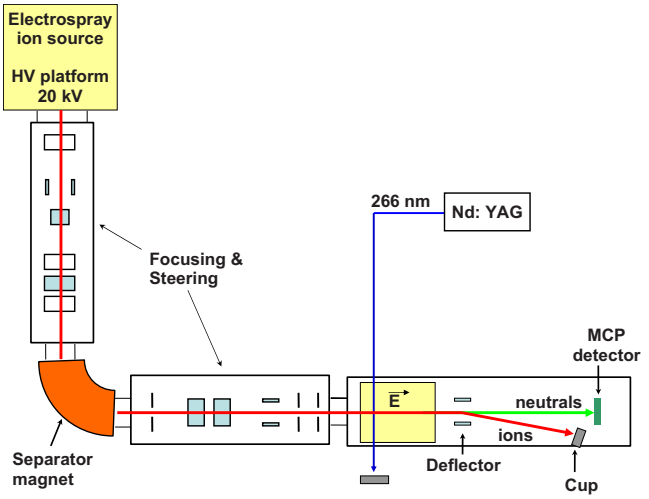

FIG. 2. (Color online) Schematic representation of the experimental setup with the ion-beam path and the laser setup.

speculative without the study of the dissociation lifetimes for both of these variants. These two variants of angiopeptides are also of importance in the light of Liftshiftz's and Weinkauf's work on fragmentation pathways in peptides. It is interesting to study the decay times given the fact that the fragmentation site is four amino acids' distance away from the excitation site (Y or Y^-).

We have performed experiments at the ELISA storage ring to study the dissociation of biomolecules [6] in the millisecond regime and complemented the studies with experiments at a different linear time-of-flight (TOF) setup to probe the dissociation in the submicrosecond regime [21]. In this paper, we present experimental studies on the dissociation lifetimes of two angiotensin peptide variants under the absorption of 266 nm UV radiation, employing the linear TOF setup. The present work sheds light on the creation of a CO_2 fragment from the two different peptides.

II. EXPERIMENTAL METHOD

The doubly deprotonated angiotensin II [[Val^5]-angio (mass=1030 amu) and [Asn^1, Val^5] (mass=1029 amu)] were produced by an electrospray-ion source. The angiotensin variants were dissolved in methanol, and ammonium hydroxide was added to obtain a pH of about 8.2. The dianions, which are formed in the gas phase, were first stored in a Paul trap with helium as the buffer gas. The trapped dianions were then extracted at the rate of 80 Hz and accelerated to 40 keV before entering a separator magnet. Figure 2 shows a schematic of the experimental setup. The mass selected dianions were electrostatically deflected by 3° from their straight path, to eliminate neutral molecules formed when the dianions on their way to the interaction region collided with residual gas.

To study the dynamics of the photodissociation that follows prompt photodetachment—in particular, the dissociation time—an electric field region, which encloses the interaction region, is applied, as shown in Fig. 3. We have earlier used this electric field region as an energy spectrometer for

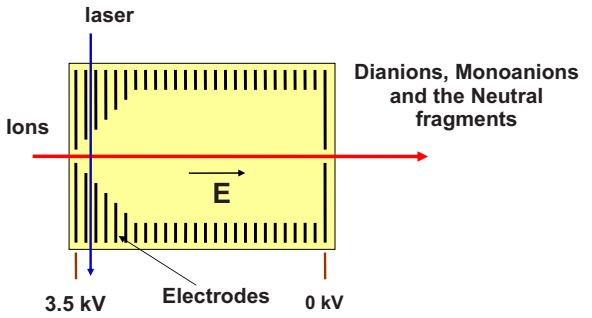

FIG. 3. (Color online) Schematic representation of the spectrometer showing the field region.

photoelectrons [22]. The fourth harmonic of a Nd:YAG laser (266 nm) was employed at a 40 Hz repetition rate. The dianions interact with the laser light at right angles about 6 cm downstream from the entrance of the spectrometer, which is about 26 cm in length. The repetition rate of the ion trap extraction was double that of the laser to enable background measurement at every alternate cycle. The entrance of the spectrometer was kept at about 3.5 kV higher than the exit, thus accelerating the dianions before they entered the spectrometer.

A stack of electrodes inside the spectrometer creates a homogeneous electric field in which anions are decelerated. The position and hence the time of dissociation of the promptly formed monoanions (see later discussion) can be gleaned from the time of flight for the neutral fragments from the point of their formation up to the particle detector. All the neutrals that are formed outside the spectrometer would have the same velocity and would be piled as a single peak with a TOF larger than those formed inside the spectrometer. The TOF is the time between the electronic signal from the laser, corresponding to the laser pulse, and the signal from the neutral particle microchannel plate (MCP). In our experiment, with an energy of 40 keV and a spectrometer voltage of 3.5 kV, dissociation times up to 2.25 μs could be resolved for the present dianions. The particles travel about 1.6 m from the exit of the spectrometer before they are detected by a microchannel plate (MCP) detector. An electrostatic deflector was employed before the particle detector to deflect ions away from their path to the MCP. In the present experiment, fragment products of the photon-dianion interaction are singly charged and neutral species. The current experimental arrangement cannot identify the mass of the detected fragments, but previous photoabsorption studies have shown that CO_2 is by far the most dominating neutral fragment [13].

III. RESULTS AND DISCUSSION

Figure 4 shows the TOF of the neutral fragments and the monoanions that are formed after the photoabsorption by [Asn, Val^5] angiopeptide dianions. The monoanion peak includes both the dissociated and the undissociated species. Our measurements on the laser-power dependence for the yield of the monoanion and the neutral fragment, for both peptide variants, agree with the earlier work [13]. The width

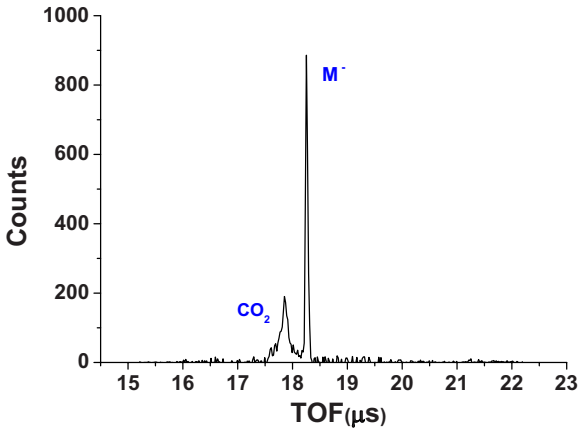

FIG. 4. (Color online) The time-of-flight spectrum for the [Asn, Val^5] angiopeptide showing both the monoanion (M^-) and the neutral (CO_2) fragments that are formed after UV photoabsorption. The neutral fragments arrive faster than the monoanions due to the spectrometer electric field. The deflector voltage (see Fig. 2) was here set to deviate only the dianions away from the MCP.

of the TOF for the monoanion peak in Fig. 4 essentially stems from the spatial width of the laser beam, the detachment lifetime, and also the ripple of the acceleration voltage. The velocity of the monoanion at the interaction region is 0.09 mm/ns and for a spatial width of the laser of about 3 mm, the estimated width of about 32 ns is very close to the experimental value, which is 31 ns. The monoanion formation is thus essentially a prompt process.

The TOF of the neutral fragments was recorded with and without the spectrometer voltage (V_{spec}). The results for the two measurements are shown in Fig. 5. The anions were deflected away from their path to the MCP for these measurements. The width of the neutral TOF spectrum stems from the kinetic energy released during the dissociation, the dissociation lifetime, and the spatial width of the laser. The kinetic energy released in the dissociation process was obtained from the width of the neutral TOF peak in a measurement with V_{spec}=0, and was determined to be 28 meV.

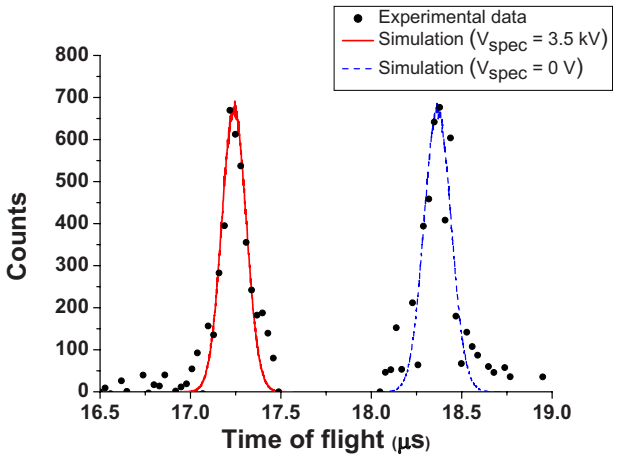

FIG. 5. (Color online) The experimental TOF distributions for the neutral photofragments (dots), from [Asn, Val^5], recorded with (solid line) and without (dashed line) electric field. The solid and the dashed lines are the Monte Carlo simulations performed with the dissociation time set to zero.

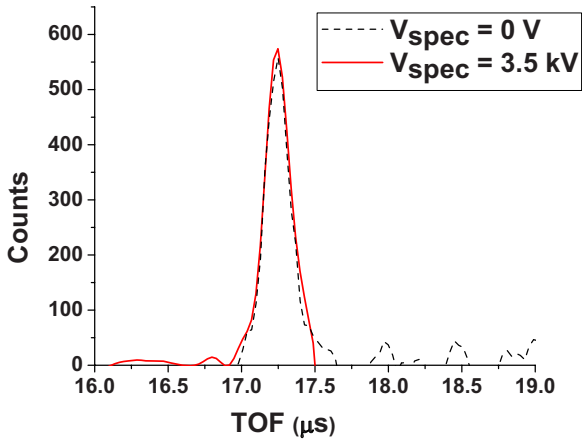

FIG. 6. (Color online) Superposition of the TOF spectra (smoothed) of the neutral photofragments, from [Asn, Val^5], obtained with the V_{spec}=3.5 kV (solid line) and V_{spec}=0 kV (dotted line). The TOF for V_{spec}=0 V is shifted to match the peak position of the TOF for V_{spec}=3.5 kV.

The TOF of the neutral fragments shifts to shorter times with the spectrometer voltage turned on, and there was no peak corresponding to dissociation occurring outside the spectrometer, which immediately shows that the dissociation is fast. Moreover, the superposition of the TOF spectra for the neutral fragments, for V_{spec}=3.5 kV and 0 V, shows no significant change in the widths related to the dissociation lifetimes, as shown in Fig. 6.

A. Monte Carlo simulations on the dissociation lifetimes

The upper limit of the dissociation time was discerned through a Monte Carlo simulation. The simulation creates random interaction events taking into consideration the spatial width of the laser and the ripple in the acceleration voltage. The TOFs of the neutral fragments were then computed assuming an exponential decay of the monoanions, taking into account the energy released in the center-of-mass frame during dissociation and its (assumed) isotropic nature. Figure 7 shows the simulated TOF spectra with different dissociation lifetimes (t_D). The simulation clearly shows that the dissociation lifetime is shorter than 100 ns.

B. Dissociation mechanism for [Asn, Val^5] angiopeptide

The present experimental results on the dissociation lifetimes together with energetics involved in the photoabsorption process lead to a better understanding of the dissociation mechanism involved in the [Asn, Val^5] angiopeptide. As mentioned previously, the yield of CO_2 was determined to be due to a two-photon process, which may be understood from the energetics of the process. The absorption of the first photon of energy 4.63 eV induces a π-π^* transition in the aromatic site of [Asn, Val^5].

The formation of the excited state in the tyrosine anion is believed to cause essentially a prompt electron emission from the phenoxy anion. The "extra" electron at the phenoxy

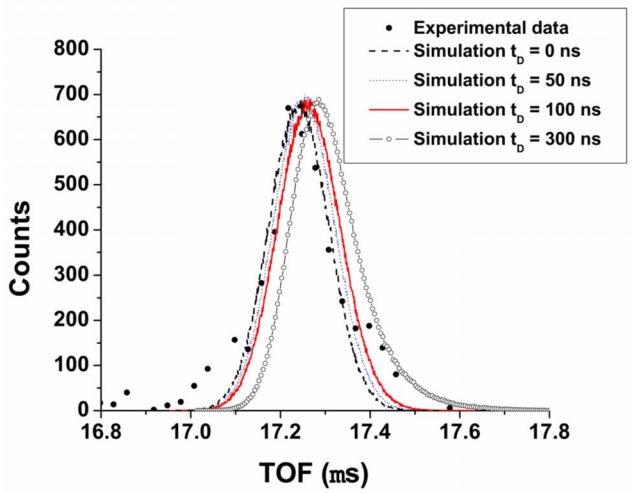

FIG. 7. (Color online) Monte Carlo simulation for the TOF of the neutral fragment from [Asn, Val^5]. The simulations were carried out for exponential dissociation times of t_D=0, 50, 100, and 300 ns.

site is more loosely bound (2.25 eV) than the one at the carboxy site (3.48 eV). We carried out a geometry optimization using GAUSSIAN 03 [23], employing the PM3 method, for the tyrosylate anion and the tyrosine radical formed postdetachment. The results show very similar geometries for the species before and after single-electron detachment. Thus, it is probable that the detached electron carries most of the remnant photon energy. The carboxylate site of the monoanion that is formed would hence be stable against detachment and dissociation. A second photon would be required to yield the CO_2 fragment. The second photon again excites the π-π^* transition, which would deexcite yielding a hot monoanion that dissociates, as shown in Fig. 8.

It is also possible to have another reaction pathway, in which the second photon detaches an electron directly from the carboxylate anion, eventually resulting in the release of CO_2. Dougard's [13] and the present experiment cannot identify this pathway as all end products are then neutral fragments.

C. TOF measurements for the Val^5 angiopeptide

We also performed the same experiment for the Val^5 peptide variant, which has two carboxylate sites (see Fig. 1). The TOF spectra of the neutral fragments, for both on and off conditions of V_{spec}, are shown in Fig. 9. The energy released in the dissociation was determined to be about 15 meV. The Monte Carlo simulation of the release of CO_2, shown in Fig. 10, indicates that the dissociation time for Val^5 is also shorter than about 100 ns. Apparently, there is an underlying

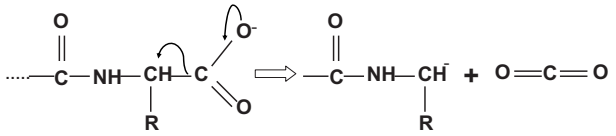

FIG. 8. Scheme for the emission of CO_2 from the photodissociation of the [Asn, Val^5] angiopeptide.

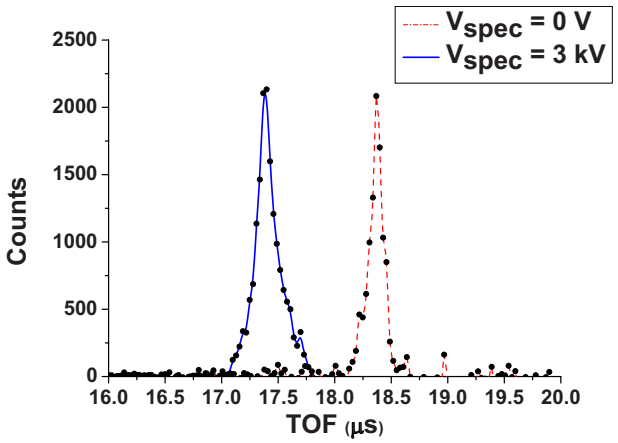

FIG. 9. (Color online) The experimental TOF distributions for the neutral photofragments (dots) from Val^5, recorded with and without the spectrometer electric field, are shown on the same time scale.

broader structure in the TOF distribution. It is symmetric and is hence not ascribed to a lifetime broadening. Rather, there may be another CO_2 dissociation channel with a higher kinetic-energy release.

The yield of CO_2 from the photodissociation of Val^5 was confirmed to be a single-photon process. In this case, the absorbed photon induces a π-π^* transition in tyrosine, which upon deexcitation yields a hot dianion that eventually detaches an electron from the carboxylate. Figure 11 depicts the release of CO_2 from the resulting monoanion.

Dougard *et al.* [13] discuss a scheme based on a charge-movement model to describe the dissociation process for [Asn^1, Val^5]. They propose the movement of a phenoxy radical to the carboxylate site, resulting in the emission of CO_2. The second photon would then be required to overcome a potential barrier associated with the movement of the radical.

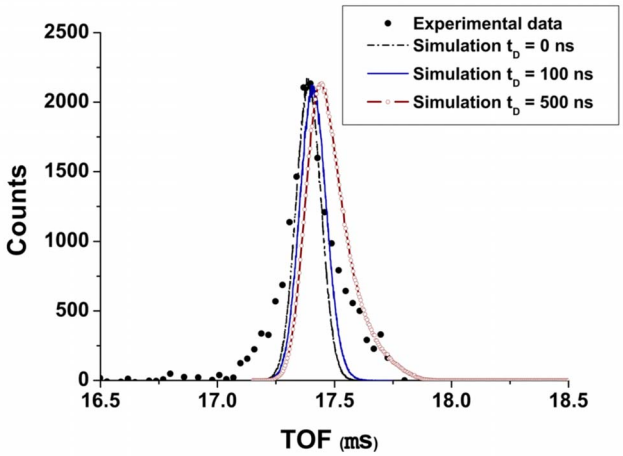

FIG. 10. (Color online) The experimental TOF distributions for the neutral photofragments (dots), from Val^5, recorded with the spectrometer electric field on. Monte Carlo simulation for the TOF of the neutral fragment from Val^5. The simulations were carried out for exponential dissociation times of t_D=0, 100 ns, and 500 ns (solid line).

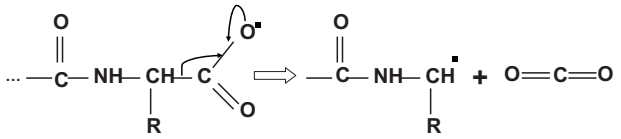

FIG. 11. Scheme for the emission of CO_2 from the photodissociation of the Val^5 angiopeptide.

However, the similarity in the dissociation lifetimes for the two variants observed in the present work, along with our results on the geometry optimization, may suggest another and simpler understanding of the dissociation process: A single-photon absorption in Val^5 may lead to electron detachment from the carboxylate anion followed by the release of CO_2. On the other hand, $[Asn, Val^5]$ first absorbs a photon that detaches an electron from the tyrosylate anion. The detached electron carries most of the remnant photon energy and hence a second photon is required to trigger the release of CO_2. Thus, according to this model, the step involved in the emission of CO_2 is similar for both the variants, which is validated by the similarity in the observed dissociation lifetimes.

IV. CONCLUSION

Photodetachment and dissociation of the $[Asn^1, Val^5]$ and the Val^5 peptide dianions were performed with 266 nm UV laser radiation. The results of a previous work [13] on the laser power dependence for the yield of monoanion and the neutral fragments was confirmed. The laser power dependence for the yield of monoanion is linear for both the peptides and was essentially a prompt process. The laser power dependence for the yield of CO_2 is linear for Val^5, while it was quadratic for the $[Asn^1, Val^5]$ peptide. The TOF spectra of the neutral fragments for both variants indicate that the dissociation is a fast process. Monte Carlo simulations were performed for the TOF of the neutral fragments and were compared to the experimental data. The results indicate that the dissociation lifetimes for both peptide dianions are shorter than 100 ns. The short decay time is interesting in light of the length of the peptide that we studied and the possible energy redistribution that is expected in such large molecules. The experimental and the geometry optimization results help us to understand the photodissociation mechanism involved and the energetics relevant to it. Thus for Val^5, a single-photon absorption may lead to electron detachment from the carboxylate followed by the release of CO_2, while $[Asn^1, Val^5]$ requires a second photon because the energy of the first photon is used to eject an electron and is hence not available for the release of CO_2.

ACKNOWLEDGMENTS

We thank S. Brøndsted Nielsen for useful discussions related to the present work. This work is supported by the Carlsberg Foundation and the Danish Research Agency (Contract No. 272-06-0427).

[1] D. P. Little, J. P. Speir, M. W. Sendko, P. B. Oconnor, and F. W. Mclafferty, Anal. Chem. **66**, 2809 (1994).
[2] R. A. Zubarev, N. A. Kruger, E. K. Fridriksson, M. A. Lewis, D. M. Horn, B. K. Carpenter, and F. W. McLafferty, J. Am. Chem. Soc. **121**, 2857 (1999).
[3] S. B. Nielsen, A. Lapierre, J. U. Andersen, U. V. Pedersen, S. Tomita, and L. H. Andersen, Phys. Rev. Lett. **87**, 228102 (2001).
[4] P. Hvelplund, B. Liu, S. B. Nielsen, S. Panja, J. C. Poully, and K. Støchkel, Int. J. Mass. Spectrom. **225**, 83 (2003).
[5] L. Lammich, M. Petersen, M. Brøndsted Nielsen, and L. H. Andersen, Biophys. J. **92**, 201 (2007).
[6] L. H. Andersen, H. Bluhme, S. Boye, T. J. D. Jørgensen, H. Krogh, I. B. Nielsen, S. Brøndsted Nielsen, and A. Svendsen, Phys. Chem. Chem. Phys. **6**, 2617 (2004).
[7] L. H. Andersen, I. B. Nielsen, M. B. Kristensen, M. O. A. El Ghazaly, S. Haacke, M. B. Nielsen, and M. A. Petersen, J. Am. Chem. Soc. **127**, 12347 (2005).
[8] C. Lifshitz, Int. J. Mass Spectrom. Ion Process. **118**, 315 (1992).
[9] R. Weinkauf, P. Schanen, D. Yang, S. Soukara, and E. W. Schlag, J. Phys. Chem. **99**, 11255 (1995).
[10] E. W. Schlag, H. L. Selzle, P. Schanen, R. Weinkauf, and R. D. Levine, J. Phys. Chem. A **110**, 8497 (2006).
[11] Y. Hu, B. Hadas, M. Davidovitz, B. Balta, and C. Lifshitz, J. Phys. Chem. A **107**, 6507 (2003).
[12] L. Joly, R. Antoine, M. Broyer, J. Lemoine, and Ph. Dugourd, J. Phys. Chem. A **112**, 898 (2008).
[13] R. Antoine, L. Joly, A. R. Allouche, M. Broyer, J. Lemoine, and Ph. Dugourd, Eur. Phys. J. D (to be published).
[14] R. Antoine, L. Joly, T. Tabarin, M. Broyer, Ph. Dugourd, and J. Lemoine, Rapid Commun. Mass Spectrom. **21**, 265 (2007).
[15] L. Joly, R. Antoine, A.-R. Allouche, M. Broyer, J. Lemoine, and Ph. Dugourd, J. Am. Chem. Soc. **129**, 8428 (2007).
[16] V. Gabelica, T. Tabarin, R. Antoine, F. Rosu, I. Compagnon, M. Broyer, E. De Pauw, and Ph. Dugourd, Anal. Chem. **78**, 6564 (2006).
[17] M. Kordel, D. Schooss, S. Gilb, M. N. Blom, O. Hampe, and M. M. Kappes, J. Phys. Chem. A **108**, 4830 (2004).
[18] X. B. Wang, C. F. Ding, and L. S. Wang, Chem. Phys. Lett. **307**, 391 (1999).
[19] R. F. Gunion, M. K. Gilles, M. K. Polak, and W. C. Lineberger, Int. J. Mass Spectrom. Ion Process. **117**, 601 (1992).
[20] E. H. Kim, S. E. Bradforth, D. W. Arnold, R. B. Metz, and D. M. Neumark, J. Chem. Phys. **103**, 7801 (1995).
[21] L. Lammich, I. B. Nielsen, H. Sand, A. Svendsen, and L. H. Andersen, J. Phys. Chem. A **111**, 4567 (2007).
[22] H. B. Pedersen, M. J. Jensen, C. P. Safvan, X. Urbain, and L. H. Andersen, Rev. Sci. Instrum. **70**, 3289 (1999).
[23] M. J. Frisch, G. W. Trucks, H. B. Schlegel, G. E. Scuseria, M. A. Robb, J. R. Cheeseman, J. A. Montgomery, Jr., T. Vreven,

K. N. Kudin, J. C. Burant, J. M. Millam, S. S. Iyengar, J. Tomasi, V. Barone, B. Mennucci, M. Cossi, G. Scalmani, N. Rega, G. A. Petersson, H. Nakatsuji, M. Hada, M. Ehara, K. Toyota, R. Fukuda, J. Hasegawa, M. Ishida, T. Nakajima, Y. Honda, O. Kitao, H. Nakai, M. Klene, X. Li, J. E. Knox, H. P. Hratchian, J. B. Cross, V. Bakken, C. Adamo, J. Jaramillo, R. Gomperts, R. E. Stratmann, O. Yazyev, A. J. Austin, R. Cammi, C. Pomelli, J. W. Ochterski, P. Y. Ayala, K. Morokuma, G. A. Voth, P. Salvador, J. J. Dannenberg, V. G. Zakrzewski, S. Dapprich, A. D. Daniels, M. C. Strain, O. Farkas, D. K. Malick, A. D. Rabuck, K. Raghavachari, J. B. Foresman, J. V. Ortiz, Q. Cui, A. G. Baboul, S. Clifford, J. Cioslowski, B. B. Stefanov, G. Liu, A. Liashenko, P. Piskorz, I. Komaromi, R. L. Martin, D. J. Fox, T. Keith, M. A. Al-Laham, C. Y. Peng, A. Nanayakkara, M. Challacombe, P. M. W. Gill, B. Johnson, W. Chen, M. W. Wong, C. Gonzalez, and J. A. Pople, GAUSSIAN 03, revision D.01 (Gaussian, Inc., Wallingford, CT, 2004).